Asian Journal of Physics
Vol. 31, No 2 (2022) 391-399
Available on: www.asianjournalofphysics.com

ap

The characteristics of the carbon nanotubes layer deposited by the electrophoretic method on a titanium substrate studied by Raman micro-spectroscopy and nanoindentation

Maria Pajda[1], Aleksandra Wesełucha-Birczyńska[2]*, Sylvia Turrell[3], Aleksandra Benko[4] and Marta Blażewicz[4]

[1]*Technolutions, Wiejska 7, 99-400 Łowicz, Poland*

[2]*Faculty of Chemistry, Jagiellonian University, Gronostajowa 2, 30-387 Kraków, Poland*

[3]*Laboratoire de Spectrochimie Infrarouge et Raman, Université des Sciences et Technologies de Lille, Lille, France*

[4]*AGH – University of Science and Technology, Faculty of Materials Science and Ceramics, Mickiewicza 30, 30-059 Kraków, Poland*

The multi-walled carbon nanotubes (MWCNT) layer deposited on the titanium surface in an electrophoretic process for 30 s and at a voltage of 30 V was investigated by Raman spectroscopy. The layer structure was analyzed by the depth scanning method. Some differences have been noticed between the top and bottom surfaces of the tested layer, i. e, at the MWCNTs / air interface and the MWCNTs / Ti interface, respectively. The MWCNTs / air interface shows the character of a graphite-like layer, probably due to the presence of shells with a large diameter, while the boundary at the interface of the MWCNTs layer with titanium indicates a characteristic of MWCNTs due to the G-band splitting and its dispersion. The observed shift of the G′-band towards the higher wavenumbers indicates a compressive strain on the layer of carbon nanotubes in contact with the titanium substrate. The measurements of the hardness of the obtained layer showed that the reaction of the material is much more plastic, because plastic work exceeds the value of elastic work up to 5 times.

Keywords: Multi-walled carbon nanotubes (MWCNTs) layer, Electrophoretic deposition (EPD), Raman micro-spectroscopy, Nanoindentation.

1 Introduction

Metals are widely used in technology, also as a substrates in various technical and medical applications due to their desired mechanical properties. For orthopedic implants, titanium is considered the most suitable, biocompatible metal [1]. Coatings on such substrates offer the possibility of modifying the surface properties in order to improve their performance or achieve the desired materials properties, including biocompatibility [2,3]. An interesting possible application of carbon nanotubes (CNTs) as a surface modifying nanophase are materials for biomedical purposes, e.g. for the use in orthopedic problems or for the construction of biosensors or electrodes for stimulating the nervous system [4-6]. While CNTs toxicity is still highly controversial, CNTs have also been proven to have osteogenic properties [7].

One of the methods of obtaining layers, which is electrophoretic deposition (EPD), is an interesting technique that allows one to create a thin conductive layer on a substrate [8]. The surface created in this way has biomimetic properties. It is also possible to tailor the deposited layer by the appropriate selection of processing parameters. From the various parameters of the EPD process, the size and concentration of the

Corresponding author
e mail: birczyns @chemia.uj.edu.pl (Aleksandra Wesełucha-Birczyńska)

particles in the suspension, the applied voltage and the time of particles deposition are of primary importance [9].

In this work, we applied Raman spectroscopy as the basic tool to determine the properties of the tested layer of carbon nanotubes. The most interesting surface topography in terms of contact with body fluids, including blood, seems to have the thickness and shape of the coating formed during the 30 s deposition [10]. Therefore, the layer deposited for the 30s at a voltage of 30V is the subject of the analysis in the current work. The mechanical properties of the layer were also presented in this work. Since the mechanical properties affect the functional capabilities of the material, these characteristics were taken and correlated with the results of the depth penetration analysis on this layer by Raman spectroscopy. This was the first time this layer had been tested with both methods.

2 Experimental

The multi-walled carbon nanotubes functionalized with OH group (MWCNTs-OH) of outside diameter 10-30 nm, inner diameter 5-10 nm, length of 1-2 μm, and more than 95% purity, were purchased from Nanostructured & Amorphous Materials, Inc., USA. A suspension was obtained by the sonication of functionalized MWCNTs-OH in ethanol, acetone and water by an ultrasound processor (Vibra-Cell, type VCX130, by Sonics & Materials, Inc, USA). The suspension prepared in this way was then used for EPD deposition in order to coat the titanium plates with dimensions of 10×10 mm. The analyzed layer (referred to as the MWCNTs) was obtained by depositing carbon nanotubes for 30 s at a voltage of 30 V with a titanium plate as a positively charged electrode. The sample was then allowed to dry under room atmosphere conditions.

Raman spectra were collected using a Renishaw inVia Raman spectrometer working in confocal mode, with 50× and 100× magnification objectives (NA = 0.50 and NA = 0.90, respectively). Various laser excitation wavelengths were used: 785 nm (1,58 eV), 514. 5 nm (2,41 eV), 473 nm (2,62 eV), and 266 nm (4,66 eV). The measurement configuration was as follows: exposure time: 10 s, accumulations: 9, laser power at the sample ~1 mW to avoid heating of the sample. Depth penetration was performed in a confocal mode using a 514.,5 nm laser line and a 100× objective. Factory-supplied software was used to analyze the spectra, e.g. the curve fit procedure to calculate the position, intensity and area of characteristic peaks (Renishaw, WiRE v. 2.0 and 3.4). The four-band model was applied in the 1750-1140 cm^{-1} range and results are presented in insets in Fig 1B. The band parameters, the positions of the component bands, their height, full width at half-height (FWHH) and percentage of the Lorentz–Gauss curve were fitted and collected in Table 1.

The dispersion of the G-, D1- and G'-peak is defined as the change in the position of the respective peak as a function of the excitation wavelength [11]:

$$Peak_{disp}\left(\frac{\mathrm{cm}^{-1}}{\mathrm{nm}}\right)=\frac{Peak_{pos}\,(266\mathrm{m})-Peak_{pos}\,(785\mathrm{m})}{(785-266)\mathrm{m}}.$$

The G- and D1- bands' dispersion for the MWCNTs layer obtained in the EPD process, at the MWCNTs/ air interface, was evaluated in the 1800-1000 cm^{-1} range using model of three bands, D1, G and D2 (Fig 2). Analysis of the MWCNTs layer during depth penetration modality was estimated applying three and two bands model for the 1800-1000 cm^{-1} and for 3200 – 2300 cm^{-1} range, respectively (Fig 3 and Table 2).

The hardness of the studied layer was tested using a Nanoindentation tester NHT3 by Anton Paar and an optical microscope with an objectives 5, ×20, ×50, and ×100. The applied maximum load was equal to 5 mN, the loading rate was increased linearly for 30s then it was stopped by 5mN for 10s and then decreased linearly for 30s.The depth range was up to 1300 nm (Table 4).

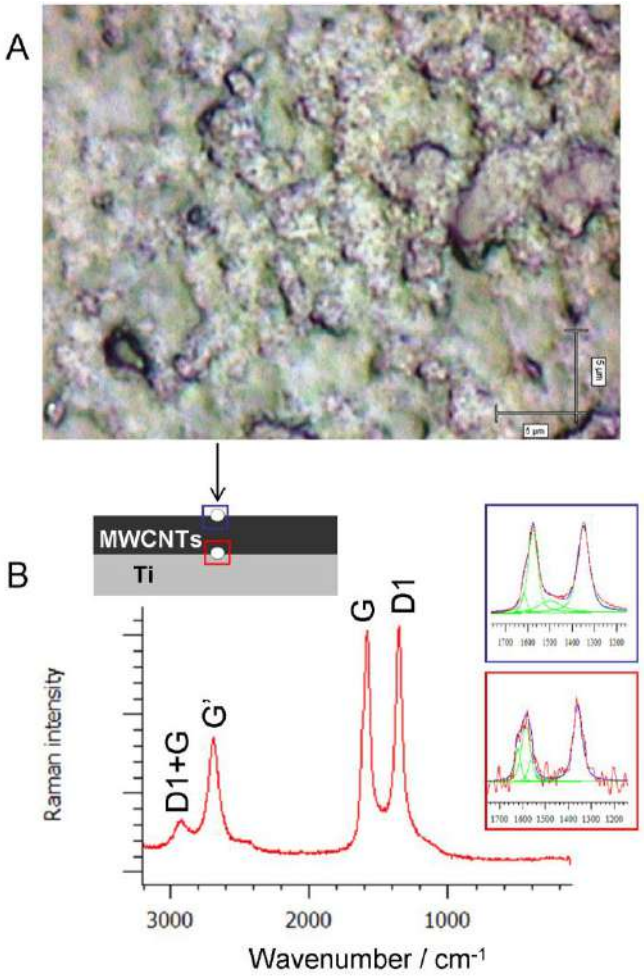

Fig 1. (A) A microphotograph showing the surface topography of the MWCNTs layer obtained in the EPD process at a voltage of 30 V, during the deposition time of 30 s; (B) Raman spectrum, 514.5 nm laser line. Insets show the Raman spectra in the 700-1200 cm^{-1} region at the MWCNTs / air and MWCNTs / titanium interfaces in the upper and lower insets, respectively. Information regarding the curve-fitted spectra are reported in Table 1.

3 Results and Discussion

3.1 The Raman micro-spectroscopy

MWCNTs nanostructures were used as a phase modifying the surface of a biocompatible titanium support. They were not harmful to the living organism [9,12]. A microphotograph of the deposited layer is presented in Fig 1A, while the Raman spectrum of its surface is shown in Fig 1B. The spectrum is characteristic of carbon materials because of its shape with typical bands [13,14]. In the visible range, the sp^2 phase cross-section is particularly well visible at 514.5 nm excitation [15,16]. The group of peaks around 1350 cm^{-1} is called the D1-band because it results from the disordering in the material [13,17,18]. This band arises from the breathing motion of sp^2 rings, so is characteristic of almost all kinds of carbonaceous materials [19]. A group of peaks due to the tangential vibrations of the carbon atoms, constituting the prominent band that appears at ca. 1600 cm^{-1} is called the G-band (G designates graphite) [14,16,17]. The poorly organized

microcrystalline graphite shows also other bands, around 1620 cm^{-1} (D2-band) due to in-plane defects and heteroatoms, and around 1500 cm^{-1} (D3-band) due to defects outside the plane of the aromatic layers [13, 20]. The Raman spectrum of single walled carbon nanotubes (SWNTs) is characterized by the presence of the G^- and the G^+ bands which correspond to the axial and circumferential vibrations of the rolled graphene sheet [15]. These results are mentioned since the interpretation of the MWCNTs Raman spectra is based on the theoretical and experimental results obtained for SWCNTs [15,17]. The number of vibrational modes that make up the G-band can be up to four [17]. Table 1 shows the resolved spectral features shown in Fig 1B inset. The relatively wide band at 1527 cm^{-1} (D3-band) and 1576 cm^{-1} (G-band) indicate a low curvature of the carbon nanotubes at the MWCNTs / air interface [21]. These bands move to 1547 cm^{-1} and 1584 cm^{-1}, respectively, and their half-widths clearly decrease, with a simultaneous relative increase in the intensity of the G-band components. These changes suggest the contribution of inner shells of MWCNTs in the formation of this interface [17].

The second-order Raman spectrum is dominated by the G′ band approximately at 2700 cm^{-1}. This band is due to the two-phonon process and is related to the possibility of an appropriate coupling effect necessary for this type of phenomenon [18]. Therefore, its intensity is particularly sensitive to the sample purity [17]. Hence this band is also especially attractive for stress monitoring [22].

Table 1. Peak positions, linewidths, heights, %Gaussian for the bands in the region 1750-1140 cm^{-1} shown in the inset in Fig 1B.

Measurement points	Position (cm^{-1})	FWHH (cm^{-1})	Height	% Gaussian	Assignments
MWCNTs / air interface	1349	66	2720	47	D1-band
	1527	136	464	45	D3-band
	1576	50	2496	49	G-band
	1617	36	776	53	D2-band
MWCNTs / Ti interface	1359	53	58	37	D1-band
	1547	51	12	44	G^--band
	1584	37	46	49	G^+-band
	1621	35	30	52	D2-band

3.2 The G- and D- band dispersion

The changes occurring in the MWCNTs layer, when the excitation wavelength changes from 266 nm to 785 nm, are shown in Fig 2, and reflects the reinforcement process. The G-band dispersion is defined as the rate of change of the G-band position as a function of the excitation wavelength (see experimental section) [11,16]. The position of the E_{2g} graphite band at 1580 cm^{-1} does not depend on the excitation of laser energy [18]. The appearance of dispersion indicates the presence of structural defects in the investigated MWCNTs layer [21]. The G-band dispersion, observed for the layer obtained from the deposited MWCNTs, is equal to 0.030 cm^{-1}/nm, and is almost 3 times smaller than that observed for other fibrous material, e.g. nonwoven carbon fibers, Fig 2A [23,24]. This proves that the studied layer is relatively well organized.

The D1-peak dispersion, calculated, analogously to the G- band dispersion, the change of the D peak position as a function of the excitation wavelength, is clearly manifested, see Fig 2B. Its attribution to an A_{1g} mode is due to a change in the selection rules for the Raman effect for some phonons between the K and M points of the Brillouin zone [13,18]. Thus, the peak results from the presence of disorder [17]. The D1-band position upshifts with increasing excitation laser energy. The contribution of all phonons around the K point in the Brillouin zone, the high dispersive acoustic phonons and optical phonons, can explain the D1-band's significant intensity. They induce dispersive character of D1-band [18]. Dispersion is expressed

in ($cm^{-1}eV^{-1}$) units. The D1-band dispersion for the studies of the MWCNTs-OH layer was evaluated as 55 cm^{-1}/eV, while 53 cm^{-1}/eV was noticed for SWCNTs [15].

The G′-band dispersion was calculated as equal to 99 cm^{-1}/eV for the MWCNTs-OH layer, while it is 106 cm^{-1}/eV for SWCNTs [15]. The G′-band dispersion is about two times greater than that observed for the disorder-induced in D-band.

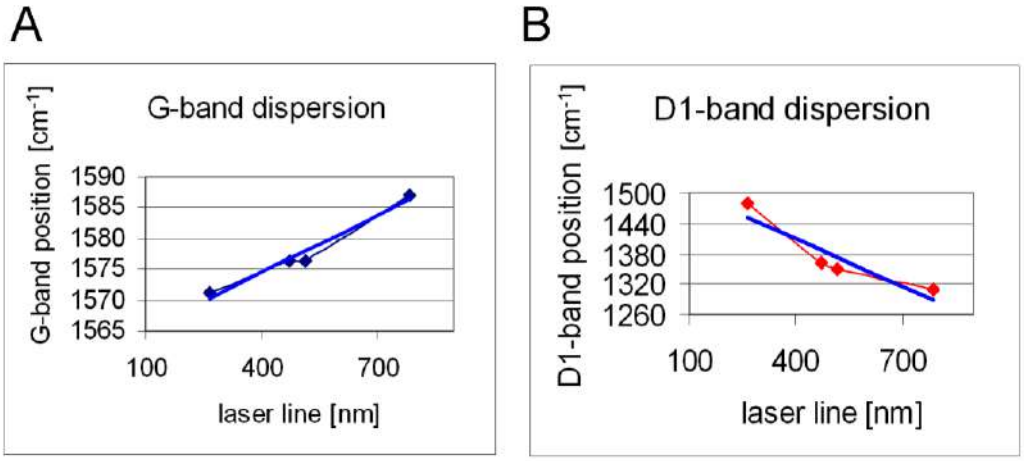

Fig 2. The G- and D- bands' positions as a function of excitation wavelength for the MWCNTs-OH layer obtained in the EPD process, the trend of the changes is marked.

3.3 The structure of the MWCNTs layer

To estimate the degree of ordering in carbon materials, several parameters are used, such as the position of the bands, their FWHH, the intensity ratio D1 / G (R1 factor) and the surface factor D1 / (G + D1) (R2 factor) [13]. In order to thoroughly investigate the characteristics of the layer deposited on the titanium substrate, appropriate measurements were carried out using the Raman spectroscopy method. Figure 3 shows the trends in the G, D1 and G' peaks positions and their FWHH for the four measurements locations in the deposited layer obtained during the Raman method depth scanning experiment for the 514.5 nm excitation.

The positions of the bands and their half-widths were determined by a curve fitting method (details are reported in the experimental section). Some differences can be noticed between the MWCNTs / air interface and the MWCNTs / Ti substrate interface, which can be correlated with the density of defects, see Table 2 [21].

The first measurement point, at the MWCNTs / air interface, indicates the characteristics of the graphite-like layer, i.e. a considerable degree of order. Its spectrum is shown in Fig 1B [21,25]. The degree of order is determined by the R2-factor estimated around 0.5. This assessment is confirmed by R1 ratio, close to 1, the lowest from all of measurements points (Table 2) [21]. For the next measurement points, in the performed depth scanning, both R2 and R1 parameters have higher values than those observed for the MWCNTs / air interface. So, it seems that the interaction of the tested layer with the titanium substrate introduces some of its stabilization. Depth profiling experiment reveals the difference in the kind of defects and their arrangement monitored by the R1 (ID/IG ratio) and also R2 factor [21].

At the MWCNTs / air interface, the G′band with a lower wavenumber (a band at around 2970 cm^{-1} dominates) indicates that in this position the sample is characterized by fine crystallites (Table 2)[21]. This is also in line with the relatively small R1 factor as previously discussed. The higher wavenumber for G′at the remaining measurement points indicates the presence of larger crystallites.

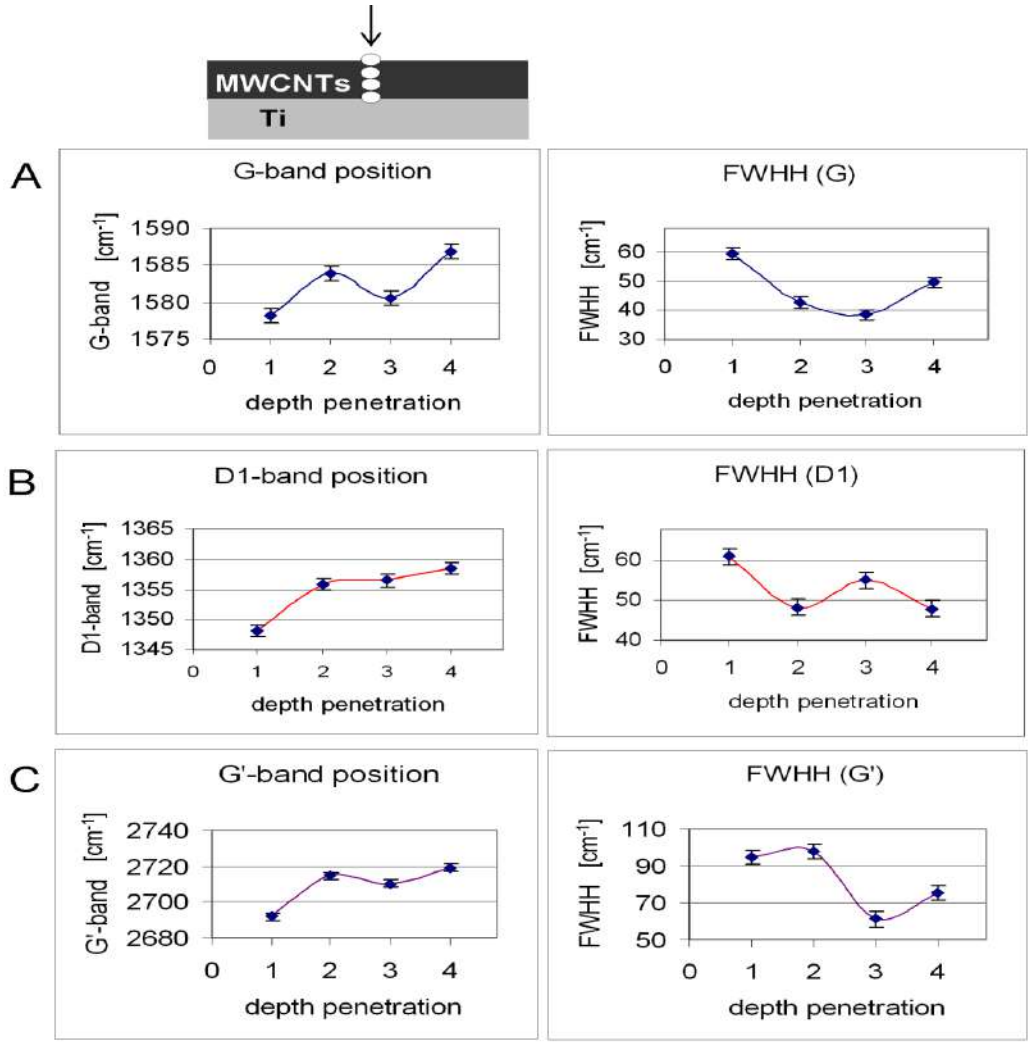

Fig 3. The position of the band and its half-width for four measurements points during depth scanning from the MWCNTs/air interface, i.e., the 1st point- is the top surface of the layer i.e, the MWCNTs / air interface, and the 4th point is the MWCMTs/Ti interface (see scheme), (A) G-band, (B) D1-band, and (C) G'-band, 514.5 nm laser line.

Table 2. The G′-band position and calculated R1 and R2 during MWCNTs layer depth profiling experiment (ID1 – intensity of D1-band, IG – intensity of G-band, AD1- area of D band, AG- area of G-band).

Measurement point	G′ (cm^{-1})	R1 (ID1/IG)	R2 (AD1/(AD1+AG+AD2))
1, MWCNTs layer/ air interphase	2691±1	1.034±0.05	0.494±0.05
2, inside layer	2714±1	1.275±0.05	0.526±0.05
3, inside layer	2710±1	1.297±0.05	0.5814 ±0.05
4, MWCNTs layer/Ti support interphase	2719±1	1.201±0.05	0.519±0.05

Additionally, a shift of the G′band is observed, as shown in Fig 3C and Table 2, which indicates the stresses that nanotubes are subjected to in the created layer. The shift towards higher wavenumbers reflects

the increasing pressure when comparing the interfaces, the MWCNT/ air layer (first measurement point) and the MWCNT layer / titanium substrate (fourth measurement point) [22]. It was assessed that the observed upward shift of 7 cm^{-1} was judged to be indicative of a 1% compressive strain [26]. In the tested layer, the observed shift towards a higher wavenumber is 28 cm^{-1}, which seems to indicate a 4% compressive strain on the layer of carbon nanotubes in contact with the titanium substrate.

3.4. The nanoindentation results

The sample surface roughness caused difficulties in measurements of the mechanical properties with the instrumented indentation technique. However, three measurements were made selecting the highest, flat spots on the surface. The Anton Paar Nano Hardness Tester NHT3 head was used to perform the measurements. A maximum 5mN load was used during the measurements. The results are displayed in Fig 4 and presented in Table 3.

Table 3. The mechanical properties of the studied MWCNTs layer.

Physical quantity*	unit	1	2	3	Mean	Std. Dev.
HIT	Mpa	125.83	133.74	167,81	142,46	22,30
EIT	Gpa	9.88	11	18,74	13,21	4,82
CIT	%	1.35	1.28	1,43	1,35	0,07
S	mN/nm	0.07	0.085	0,12	0,09	0,02
W_{elast}	pJ	220.07	210.90	205,62	212,19	7,31
W_{plast}	pJ	1082.01	971.74	1158,90	1070,88	94,07
W_{total}	pJ	1302.08	1182.65	1364,52	1283,08	92,41

*HIT - instrumented hardness in MPa; EIT - instrumented Young Modulus in GPa; CIT -instrumented creep in %; S - stiffness in mN/nm; W_{elast} - elastic work during indentation in pJ; W_{plast} - plastic work during indentation in pJ; W_{total} - elastic work and plastic work added together, in pJ.

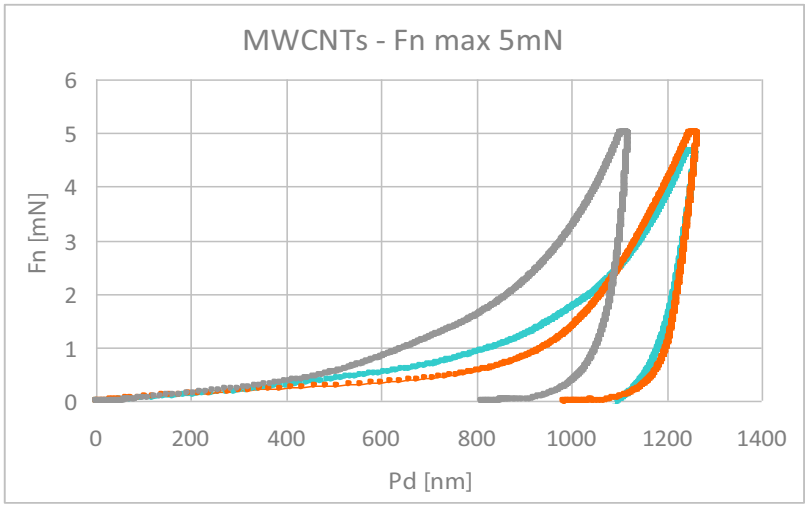

Fig 4. The loading/unloading curves for the studied MWCNTs EPD (30V, 30s) layer; force Fn (mN) *vs* penetration depth Pd (nm).

The measurements showed that the material's response was much more plastic than elastic. The plastic work was 5 times bigger than the elastic work during measurements, which can be seen on the plot: the plastic work is the area between the loading and unloading curves. The elastic work is the area under the unloading curve (Fig 4). The hardness and Young Modulus were the biggest during the 3rd measurement. However, both the hardness and Young modulus have rather small values as well as creep.

4 Conclusions

An interesting carbon layer made of carbon nanotubes on a titanium substrate in the EPD deposition process was studied. The Raman spectroscopy mode depth profiling allowed to characterize the structure of this layer. The outer surface shows the nature of the graphite layer. Nanostructures in the layer at the interface of carbon nanotubes and titanium, manifest the character typical of carbon nanotubes. Additionally, multi-wavelengths measurements allowed the assessment of the dispersion of the G- and D- bands, which are indicators of the disorder observed in the studied layer. The noticed G′ band shift towards higher wavenumbers signifies a compressive strain on the layer of carbon nanotubes in contact with the titanium support. The nanoindentation measurements of the obtained layer show that the material is rather plastic, because the value of plastic work exceeds the value of elastic work up to 5 times.

References

1. Anderson P J, Comprehensive Biomaterials, (Elsevier, Amsterdam), 2011, p 5.
2. Sorrell C C, Taib H, Palmer T C, Peng F, Xia Z, Wie M, Biological and Biomedical Coatings Handbook Processing and Characterization, (CRC Press, USA), 2011, p 82.
3. Karthik B M, Gowrishankar M C, Sharma S, Hiremath P, Shettar M, Shetty N, Coated and uncoated reinforcements metal matrix composites characteristics and applications – A critical review, *Cogent Eng*, 7(2020)1856758; doi.org/10.1080/23311916.2020.1856758.
4. Han Z J, Rider A E, Fisher C, van der Laan T, Kumar S, Levchenko I, Ostrikov K, Carbon Nanotubes and Graphene, (Elsevier, Amsterdam), 2014, p 279.
5. Munir K S, Wen C, Li Y, Carbon nanotubes and graphene as nanoreinforcements in metallic biomaterials: a review, *Adv Biosyst*, 3 (2019) 1800212; doi. 10.1002/adbi.201800212.
6. Frączek-Szczypta A, Dlugoń E, Wesełucha-Birczyńska A, Nocuń M, Błażewicz M, Multi walled carbon nanotubes deposited on metal substrate using EPD technique. A spectroscopic study, *J Mol Struct*, 1040(2013)238–245.
7. Shvedova A A, Kisin E R, Porter D, Schulte P, Kagan V E, Fadeel B, Castranova V, Mechanisms of pulmonary toxicity and medical applications of carbon nanotubes: two faces of Janus?, *Pharmacol Ther*, 121(2009)192–204.
8. Boccaccini A R, Cho J, Roether J A, Thomas B J C, Minay E J, Shaffer M S P, Electrophoretic deposition of carbon nanotubes, *Carbon*, 44 (2006)3149–3160.
9. Benko A, Przekora A, Wesełucha-Birczyńska A, Nocuń M, Ginalska G, Błażewicz M, Fabrication of multi-walled carbon nanotube layers with selected properties via electrophoretic deposition: physicochemical and biological characterization, *Appl Phys A*, 122(2016)447; doi.org/10.1007/s00339-016-9984-z.
10. Wesełucha-Birczyńska A, Stodolak-Zych E, Piś W, Długoń E, Benko A, Błażewicz M, A model of adsorption of albumin on the implant surface titanium and titanium modified carbon coatings (MWCNT-EPD). 2D correlation analysis, *J Mol Struct*, 1124(2016)61–70.
11. Ferrari A C, Robertson J, Raman spectroscopy of amorphous, nanostructured, diamond–like carbon, and nanodiamond, *Phil Trans Roy Soc Lond*, 362(2004)2477; doi.org/10.1098/rsta.2004.1452.
12. Wesełucha-Birczyńska A, Stodolak-Zych E, Turrell S, Cios F, Krzuś M, Długoń E, Benko A, Niemiec W, Błażewicz M, Vibrational spectroscopic analysis of a metal/carbon nanotube coating interface and the effect of its interaction with albumin, *Vib Spectrosc*, 85(2016)185–195.
13. Beyssac O, Goffe B, Petitet J-P, Froigneux E, Moreau M, Rouzaud J-N, On the characterization of disordered and heterogeneous carbonaceous materials by Raman spectroscopy, *Spectrochim Acta*, A59(2003)2267–2276.

14. Heise H M, Kuckuk R, Ojha A K, Srivastava A, Srivastava V, Asthanac B P, Characterisation of carbonaceous materials using Raman spectroscopy: a comparison of carbon nanotube filters, single- and multi-walled nanotubes, graphitised porous carbon and graphite, *J Raman Spectrosc*, 40(2009)344–353.
15. Dresselhaus M S, Dresselhaus G, Saito R, Jorio A, Raman spectroscopy of carbon nanotubes, *Phys Rep*, 409 (2005) 47–99.
16. Ferrari A C, Robertson J, Interpretation of Raman spectra of disordered and amorphous carbon, *Phys Rev B*, 61(2000)14095; doi.org/10.1103/PhysRevB.61.14095.
17. Lehman J H, Terrones M, Mansfield E, Hurst K E, Meunier V, Evaluating the characteristics of multiwall carbon nanotubes, *Carbon*, 49(2011)2581_2602.
18. Matthews M J, Pimenta M A, Dresselhaus G, Dresselhaus M S, Endo M, Origin of dispersive effects of the Raman D band in carbon materials, *Phys Rev B*, 59(1999)R6585; doi.org/10.1103/PhysRevB.59.R6585.
19. Ferrari A C, Robertson J, Resonant Raman spectroscopy of disordered, amorphous, and diamondlike carbon, *Phys Rev B*, 64(2001)075414; doi.org/10.1103/PhysRevB.64.075414.
20. Wesełucha-Birczyńska A, Babeł K, Jurewicz K, Carbonaceous materials for hydrogen storage investigated by 2D Raman correlation spectroscopy, *Vib Spectrosc*, 60(2012)206–211.
21. Antunes E, Lobo A O, Corat E J, Trava-Airoldi V, Martin A, Verissimo C C, Comparative study of first- and second-order Raman spectra of MWCNT at visible and infrared laser excitation, *Carbon,* 44(2006)2202–2211.
22. Cooper C A, Young R J, Halsall M, Investigation into the deformation of carbon nanotubes and their composites through the use of Raman spectroscopy, *Composites A*, 32(2001)401–411.
23. Wesełucha-Birczyńska A, Długoń E, Kołodziej A, Bilska A, Sacharz J, Błażewicz M, Multi-wavelength Raman microspectroscopic studies of modified monwoven carbon scaffolds for tissue engineering applications, *J Mol Struct*, 1220(2020) 128665; doi.org/10.1016/j.molstruc.2020.128665.
24. Wesełucha-Birczyńska A, Morajka K., Stodolak-Zych E, Długoń E, Dużyja M, Lis T, Gubernat M, Ziąbka M, Błażewicz M, Raman studies of the interactions of fibrous carbon nanomaterials with albumin, *Spectrochim Acta A*, 196(2018)262-267.
25. Jorio A, Pimenta M A, Souza Filho A G, Saito R, Dresselhaus G, Dresselhaus M S, Characterizing carbon nanotube samples with resonance Raman scattering , *New J Phys,* 5 (2003)139.1–139.17.
26. Zhao Q, Wagner H D, Raman spectroscopy of carbon–nanotube–based composites, *Phil Trans R Soc Lond A,* 362(2004)2407–2424.

[Received:15.11.2021; accepted: 23.12.2021]